Spike Detection Performance of a Noise-Enhanced Nonlinear Filter Across Varied Neuron Distances

Cihan Berk Güngör
Texas Instruments, Inc.
Santa Clara, CA USA
c-gungor@ti.com

Hakan Töreyin
Electrical and Computer
Engineering Department
San Diego State University
San Diego, CA USA
htoreyin@sdsu.edu

***Abstract*— The objective of this study is to assess the spike detection performance of a nonlinear filter (NF) using stochastic resonance and subsequent hard thresholding. The evaluation is based on the distance of neural spikes from the electrode. The F1 score variation of the algorithm is examined using two synthetic datasets generated with MEArec and Neurocube extracellular neural recording synthesis tools. In the MEArec recording, the algorithm achieved a 75% F1 score for spikes up to 70 µm, and in the Neurocube recording, it reached 95 µm. This contrasts with three popular unsupervised intracortical neural spike enhancement algorithms, which achieve the same F1 performance only within a 50 µm range. These results suggest that the NF spike enhancement method has the potential to increase the detectable spikes by a single electrode in resource-limited implantable intracortical neural recording systems, where hardware complexity is a critical design consideration.**

Keywords*— *intracortical neural spike detection, detection distance, nonlinear filtering, stochastic resonance

I. Introduction

Detecting neural spikes in intracortical recordings is critical for systems using electrodes in brain-machine interfaces [1] and neuroscience studies [2]. Typically, raw electrical recordings undergo analog signal conditioning to enhance neural spikes and suppress noise. After spike detection, spikes are often sorted by their source neurons before higher-level processing decodes brain activity to infer intention. Alternatively, intentions can be decoded directly from detected spikes [3]. In both cases, with or without spike sorting, the number of detected spikes affects the accuracy and efficiency of neural monitoring systems, with an electrode theoretically detecting spikes from neurons within ~140 µm, or about 1000 neurons in the rat cortex [4]. Detecting numerous spikes provides a detailed view of neural activity but increases hardware complexity and power consumption in high-density multielectrode arrays (HD-MEAs) [5]. Maximizing the number of spikes detected by a single electrode can reduce the number of channels in HD-MEAs, providing greater design flexibility for meeting the stringent requirements of implantable neural monitoring applications [6].

In [7], a spike enhancement algorithm based on a nonlinear filter (NF) that facilitates stochastic resonance has been shown to demonstrate *signal-to-noise ratio (SNR) enhancements* of spikes from distant neurons. However, the study did not delve into a critical performance aspect in neural recording applications - *spike detection performance* with distance. In this study, we evaluate how the NF method's spike detection performance varies with the distance of neural spikes from the electrode. We use NF for spike enhancement in a threshold-based detection approach and compare the results with three commonly used unsupervised spike detection techniques.

This work was supported by the National Science Foundation under Grant Number 1916160.

II. Methods

A. Nonlinear filtering (NF)

This spike enhancement method aims to leverage stochastic resonance phenomenon, where additive noise on a weak signal counterintuitively improves detectability of the weak signal [8]. Following [7], this study investigates a nonlinear filter (NF) based on the underdamped dynamics of a particle inside a monostable potential well when the particle is introduced with a force proportional to the noisy neural recording (Figure 1). Here, the particle is under the influence of two forces; one being the input noisy intracortical signal, $s_n(t)$, and the other being the force that the well potential exerts to move the particle towards the stable point in proportion to the local slope as $-dU(x(t))/dx$. The output of the system is the position of the particle projected on the x-axis, $x(t)$. In the presence of a spike, the particle could move towards walls of the potential well. However, during noise-only portions, the particle swings around the stable point. The movement of the particle in this system is governed by the generalized Langevin equation [9], which maps the two forces of the system to the acceleration and velocity of the particle: $(d^2x(t))/(dt^2) + \gamma\, dx(t)/dt = -dU(x)/dx + s_n(t)$, where γ is the damping coefficient and $U(x) = \mathrm{a}x^2/2 + \mathrm{b}x^4/4$ is the well potential with $a, b > 0$. The selection of the equation parameters of a, b, γ and the numerical solver step size are performed through a three-step parametric search, aiming to maximize the SNR improvement. The details of this process are explained in [7], but are excluded in this work for brevity. Then, the Langevin equation is solved numerically using the fourth-order Runge-Kutta method.

B. Compared spike-enhancement algorithms

The spike enhancement and detection performance of the NF is compared against three algorithms, namely band-pass filtering (BPF), discrete wavelet transform (DWT), and smoothed Teager energy operator (STEO). The selection of the algorithms was based on two criteria. Firstly, these algorithms are widely used

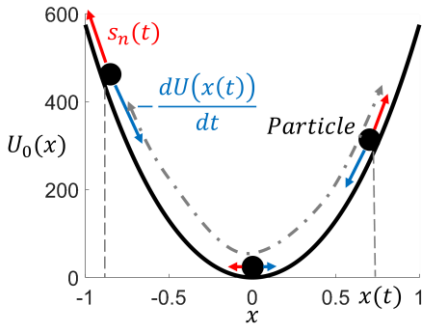

Figure 1. Nonlinear filtering method filters the noisy neural recording, $s_n(t)$ exerted as force onto a particle inside an underdamped monostable well potential. The well also exerts a force, $-\frac{dU_0(x)}{dx}$. The position of the particle projected on the x-axis, $x(t)$, is the NF output.

in spike detection, with an established history [10], [11] and broad adoption in studies inferring brain states from detected spikes [3]. Secondly, they are unsupervised methods, featuring a spike enhancement followed by a detection stage, allowing for data-independent, objective comparisons without requiring training data. Unlike some unsupervised methods like *Wave_clus* [12], they do not consider spike waveform shape, making them suitable for applications that directly decode detected spikes without a sorting stage.

Band-pass filtering aims to remove the low- and high-frequency undesired content (e.g., local field potential and noise). To minimize complexity, a 4th order finite impulse response (FIR) band-pass filter with Kaiser window is implemented in this study. The bandwidth of the band-pass filter is selected to match the neural spike band of [300 Hz – 6 kHz].

Discrete wavelet transform (DWT) is a time-frequency analysis method that decomposes signals into a set of wavelets. It operates by convolution of the signal and a mother wavelet function to obtain the information on different frequency sub-bands, while preserving their temporal information. In this study, the *sym4* is selected as mother wavelet, widely recognized in literature for its effectiveness in enhancing intracortical recordings [13].

The smoothed Teager energy operator (STEO) algorithm aims to improve the SNR of the neural signal by extracting time-frequency information of spikes without *a priori* information. The discrete-time Teager energy operator (TEO) is given as: $\psi(x[n]) = x^2[n] - x[n+1] \cdot x[n-1]$, where $x[n]$, $x[n+1]$, and $x[n-1]$ are the n^{th}, $n+1^{th}$ and $n-1^{th}$ samples of a signal. To overcome the issue of experiencing a degraded spike detection performance in low SNR and/or high noise peak scenarios, the $\psi(x[n])$ is smoothed via a Hamming window FIR filter with length 5 and the difference factor of 1, which lead to the following window filter coefficients: $w(n) = [0.08\ 0.54\ 1\ 0.54\ 0.08]$ [14].

C. Spike detection by hard thresholding

All spike enhancement methods are followed by a thresholding stage to identify the spikes. Each method employs a hard threshold set at 4 times the standard deviation (σ) of the noise in the spike enhancement stage output [10]. The noise standard deviation is accurately determined by utilizing spike enhancement stage output portions without neural spikes.

D. Synthetic recordings

The algorithms are assessed using synthetic recordings, offering known spike time points and neuron locations around the electrode. The recordings are generated by *MEArec* [15] and *Neurocube* [16], simulating a single-channel intracortical scenario with 300 neurons around the electrode. *MEArec* models cortical layer 5 with four pyramidal cells. *Neurocube* includes 4 pyramidal and 1 interneuron cells in cortical layer 5. Both tools randomly select 30 neurons from the available pool and position them around the electrode. The noise level is set at 10 µV for background noise caused by distant neurons, in line with [15], [16]. Ten single-channel intracortical recordings simulate 300 neurons for 30 seconds, combining to form the complete recording. Figure 2 presents 500 ms segments of the recordings.

E. Spike detection performance assessment

The spike detection performances of the algorithms are evaluated using true spike points. Evaluation involves extracting the numbers of true positives (TP), false negatives (FN), and false positives (FP) from the algorithm outputs. Three metrics, sensitivity (Se), positive predictivity ($+P$), and F1 score ($F1$), are then calculated as: $Se = TP/(FN + TP) * 100$, $+P = TP/(FP + TP) * 100$, $F1 = (2 * Se * (+P))/(Se + (+P))$.

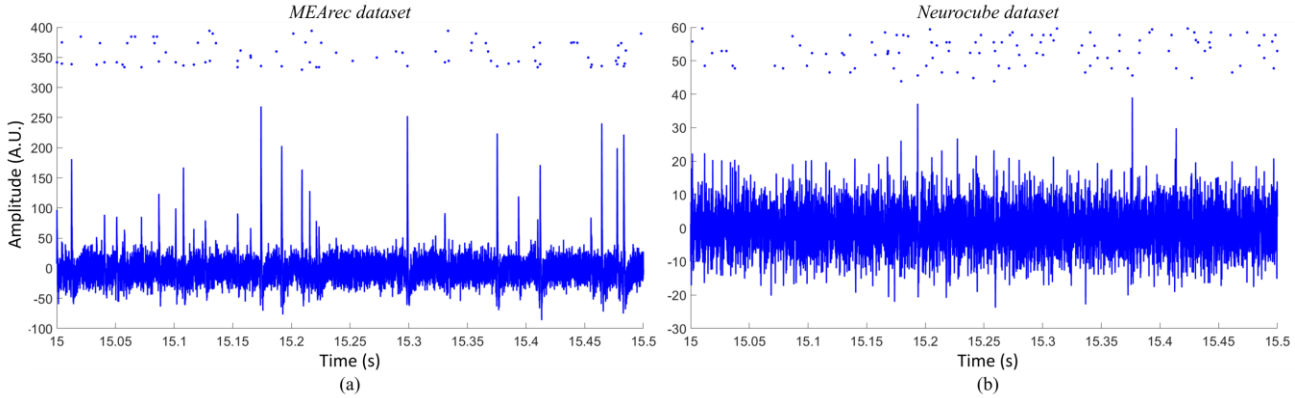

Figure 2. 500 ms portions of (a) *MEArec* and (b) *Neurocube* recordings. Blue dots positioned at the top indicate spike events, and a greater horizontal level of the dots corresponds to a higher distance of the originating neuron from the electrode.

III. Results

Figure 3 shows the outputs of the four spike enhancement methods for a 200 ms synthetic recording generated by the MEArec tool. The top plot displays the raw recording with true spikes indicated by dots. In this representative data, the NF achieves better signal improvement for the TPs and a better noise suppression. Specifically, the NF, BPF, DWT, and STEO, result in SNR improvement, ΔSNR, of 22.38dB, 3.8dB, 4.38dB, and 13.36dB, respectively. While large ΔSNR does not necessarily translate into high $F1$, for this representative portion of a single recording, the NF resulted in an $F1$ score of 65.31%, which is better than that of the BPF (34.28%), DWT (50%), and STEO (48.88%).

To assess the detection performance with respect to distance, first, $F1$ score for a neuron is calculated by considering all spikes generated by that neuron in a recording. The process is repeated for all neurons. $F1$ scores of all neurons for both recordings are shown in Figure 4. To elucidate the trend of detection performance variation with respect to distance, the spikes are categorized into groups based on the distances of their source neurons from the electrode, with each group spanning a range of 10 µm. In Figure 4, the median $F1$ scores and the standard deviations for the 10 µm distance windows are also given for both datasets.

For the *MEArec* recording, all four methods achieve $F1$ scores greater than 85% for neurons that are less than 40 µm away, which decrease with distance. Next, the maximal distance at which the algorithms can detect neuronal spikes is evaluated. An F1 score above 75% is considered satisfactory, determined by setting acceptable Se and $+P$ thresholds at 90% and 65%, respectively. A higher threshold for Se is chosen to maximize the benefit of accurately detecting neuronal spikes, while minimizing false negatives, to reduce information loss for subsequent algorithms [17]. The NF algorithm achieves median $F1$ scores above 75% at greater distances compared to other algorithms in both datasets. Specifically, while the BPF, DWT, and STEO algorithms fall below the 75% threshold for neurons beyond approximately 50 µm, the NF algorithm maintains $F1$ scores above 75% for neurons within distances of less than 70 µm and 95 µm for the *MEArec* and *Neurocube* recordings, respectively.

A potential factor contributing to the improved spike detection performance of the NF could be the beneficial role of an optimal level of noise in spike enhancement [7]. It should be noted that, to facilitate SR, the NF parameters are optimally chosen based on the recordings, following the parameter search in [7]. In contrast, BPF, DWT, and STEO lack established literature methods for recording-specific parameter optimization (e.g., BPF cutoffs, wavelet type), resulting in parameter selection based on prior work. It is noteworthy that the F1 score for untufted pyramidal cell spikes, represented by triangles (Δ) in Figure 4, consistently falls below the 75% threshold at shorter distances compared to other neuron types. Although these neuron spikes are also less effectively detected by the other methods, the interplay between the NF parameters and spike morphologies require further exploration, which is left as a future work. Furthermore, it is important to note a limitation of the study wherein synthetic recordings are utilized instead of real neural recordings. This decision is made due to the challenges of accurately localizing the source neuron in a real neural recording. While the actual distances required to achieve satisfactory $F1$ scores of 75% may differ from the results presented in this study, it is anticipated that the performance comparisons among the four algorithms would remain consistent. The superior spike detection performance of the NF for distant neurons, compared to BPF, DWT, and STEO, increases the number of neurons a single electrode can capture, reducing the number of required electrodes for the same volume. Additionally, the filter is suitable for ultra-low power implantable neural recording applications, where low-latency spike detection is critical. As a 2nd order ordinary differential equation, the NF can be efficiently implemented using analog signal processing methods, achieving both ultra-low power operation and real-time detection, as demonstrated in [18].

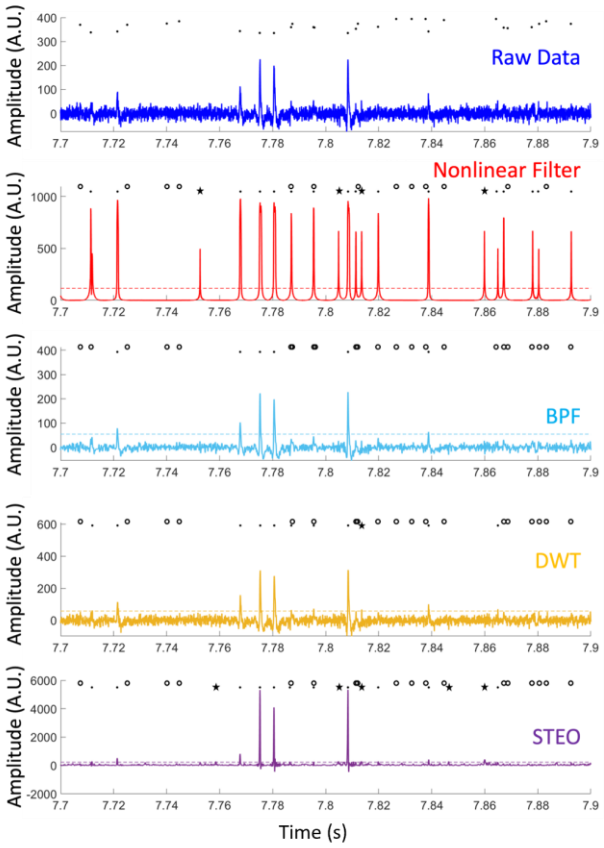

Figure 3. A 200 ms portion of the *MEArec* recording and outputs of the nonlinear filter (NF) and the compared spike enhancement methods. True-detected spikes are indicated by dots, missed spikes are denoted by hollow circles, and false-detected spikes are represented by stars.

IV. Conclusion

Unsupervised spike detection algorithms are crucial in intracortical brain monitoring for their automatic detection without training data. This study objectively evaluates a nonlinear filter (NF) and three widely-used unsupervised algorithms regarding spike detection performance across varying distances of originating neurons. Results from two synthetic neural recording datasets indicate that the NF consistently outperforms band-pass filtering, discrete wavelet

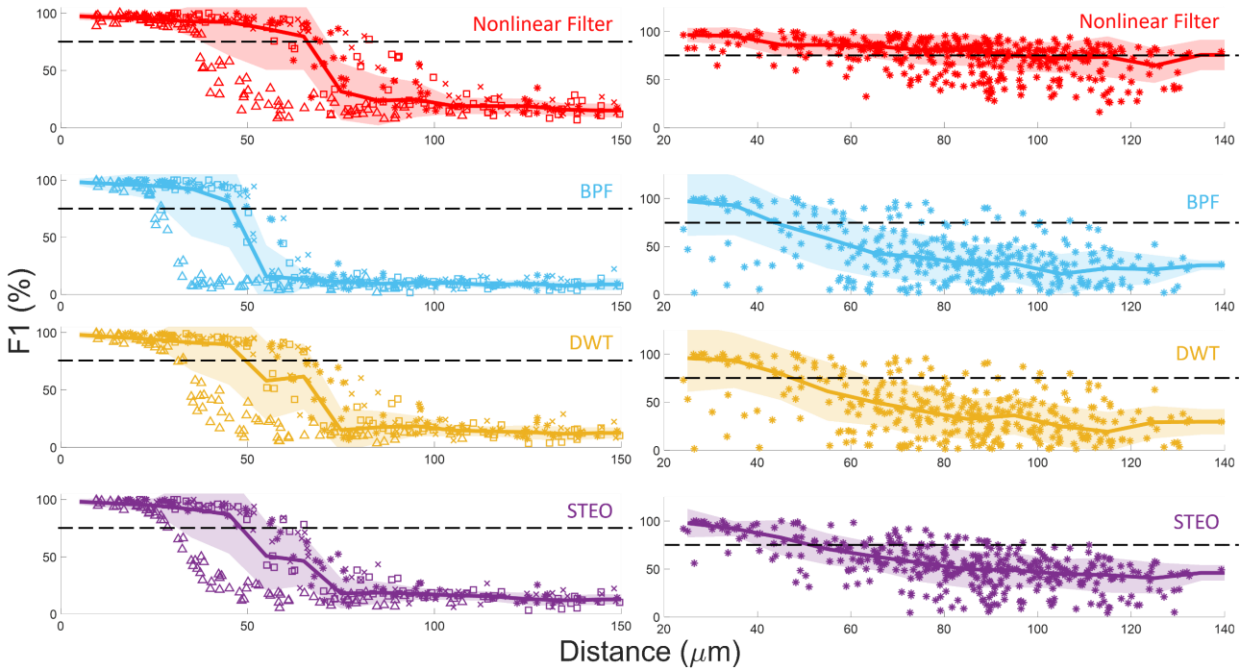

Figure 4. $F1$ scores for all 300 neurons against the distance of each neuron to the electrode. Each marker indicates the $F1$ score obtained based on all spikes of a unique neuron and the distance of the neuron. Median $F1$ and variance values are respectively presented as solid lines and shaded areas. The threshold of 75% $F1$ score is annotated with dashed lines. (Left column) *MEArec* recording. Each type of neuron is represented by a distinct marker; a star (∗), a cross (x), a square (□), and a triangle (Δ). (Right column) *Neurocube* recording.

transform, and smoothed Teager energy operator in detecting spikes from distant neurons. These findings highlight the potential of the noise-enhanced NF to maximize the detectable region within an intracortical neural recording application.

References

[1] J. Dai *et al.*, "Reliability of motor and sensory neural decoding by threshold crossings for intracortical brain–machine interface," *J. Neural Eng.*, vol. 16, no. 3, p. 036011, Apr. 2019, doi: 10.1088/1741-2552/ab0bfb.

[2] G. Buzsáki, "Large-scale recording of neuronal ensembles," *Nat Neurosci*, vol. 7, no. 5, Art. no. 5, May 2004, doi: 10.1038/nn1233.

[3] G. W. Fraser, S. M. Chase, A. Whitford, and A. B. Schwartz, "Control of a brain–computer interface without spike sorting," *J. Neural Eng.*, vol. 6, no. 5, p. 055004, Sep. 2009, doi: 10.1088/1741-2560/6/5/055004.

[4] D. A. Henze, Z. Borhegyi, J. Csicsvari, A. Mamiya, K. D. Harris, and G. Buzsáki, "Intracellular Features Predicted by Extracellular Recordings in the Hippocampus In Vivo," *Journal of Neurophysiology*, vol. 84, no. 1, pp. 390–400, Jul. 2000, doi: 10.1152/jn.2000.84.1.390.

[5] "Neuropixels 2.0: A miniaturized high-density probe for stable, long-term brain recordings." Accessed: Jul. 22, 2022. [Online]. Available: https://www.science.org/doi/full/10.1126/science.abf4588

[6] A. Marblestone* *et al.*, "Physical principles for scalable neural recording," *Frontiers in Computational Neuroscience*, vol. 7, 2013, Accessed: May 16, 2022. [Online]. Available: https://www.frontiersin.org/article/10.3389/fncom.2013.00137

[7] C. B. Güngör, P. P. Mercier, and H. Töreyin, "Investigating well potential parameters on neural spike enhancement in a stochastic-resonance pre-emphasis algorithm," *J. Neural Eng.*, vol. 18, no. 4, p. 046062, May 2021, doi: 10.1088/1741-2552/abfd0f.

[8] L. Gammaitoni, P. Hänggi, P. Jung, and F. Marchesoni, "Stochastic resonance," *Rev. Mod. Phys.*, vol. 70, no. 1, pp. 223–287, Jan. 1998, doi: 10.1103/RevModPhys.70.223.

[9] S. Lu, Q. He, and F. Kong, "Effects of underdamped step-varying second-order stochastic resonance for weak signal detection," *Digital Signal Processing*, vol. 36, pp. 93–103, Jan. 2015, doi: 10.1016/j.dsp.2014.09.014.

[10] R. Q. Quiroga, Z. Nadasdy, and Y. Ben-Shaul, "Unsupervised Spike Detection and Sorting with Wavelets and Superparamagnetic Clustering," *Neural Computation*, vol. 16, no. 8, pp. 1661–1687, Aug. 2004, doi: 10.1162/089976604774201631.

[11] S. Mukhopadhyay and G. C. Ray, "A new interpretation of nonlinear energy operator and its efficacy in spike detection," *IEEE Transactions on Biomedical Engineering*, vol. 45, no. 2, pp. 180–187, Feb. 1998, doi: 10.1109/10.661266.

[12] F. J. Chaure, H. G. Rey, and R. Quian Quiroga, "A novel and fully automatic spike-sorting implementation with variable number of features," *Journal of Neurophysiology*, vol. 120, no. 4, pp. 1859–1871, Oct. 2018, doi: 10.1152/jn.00339.2018.

[13] V. Shalchyan, W. Jensen, and D. Farina, "Spike Detection and Clustering With Unsupervised Wavelet Optimization in Extracellular Neural Recordings," *IEEE Transactions on Biomedical Engineering*, vol. 59, no. 9, pp. 2576–2585, Sep. 2012, doi: 10.1109/TBME.2012.2204991.

[14] H. Semmaoui, J. Drolet, A. Lakhssassi, and M. Sawan, "Setting Adaptive Spike Detection Threshold for Smoothed TEO Based on Robust Statistics Theory," *IEEE Transactions on Biomedical Engineering*, vol. 59, no. 2, pp. 474–482, Feb. 2012, doi: 10.1109/TBME.2011.2174992.

[15] A. P. Buccino and G. T. Einevoll, "MEArec: A Fast and Customizable Testbench Simulator for Ground-truth Extracellular Spiking Activity," *Neuroinform*, vol. 19, no. 1, pp. 185–204, Jan. 2021, doi: 10.1007/s12021-020-09467-7.

[16] L. A. Camuñas-Mesa and R. Q. Quiroga, "A Detailed and Fast Model of Extracellular Recordings," *Neural Computation*, vol. 25, no. 5, pp. 1191–1212, May 2013, doi: 10.1162/NECO_a_00433.

[17] Z. Zhang, O. W. Savolainen, and T. G. Constandinou, "Algorithm and hardware considerations for real-time neural signal on-implant processing," *J. Neural Eng.*, vol. 19, no. 1, p. 016029, Feb. 2022, doi: 10.1088/1741-2552/ac5268.

[18] L. Yang and H. Töreyin, "A 311 nW Integrated Neural Amplifier and Spike Enhancement Filter Achieving 98.99% Spike Detection Sensitivity," accepted for presentation at the 2024 IEEE International Midwest Symposium on Circuits and Systems (MWSCAS), pp. 1–5.